

Preparation and characterization of asymmetric polyethersulfone nanofiltration membranes: The effects of polyvinylpyrrolidone molecular weights and concentrations

Wenyao Shao,¹ Shenghua Wu,^{1,2} Zhuan Hong,² Qiuquan Wang,³ Ying Xiong,⁴ Ruizao Yi,² Quanling Xie,^{2,3} Zongyuan Xiao¹

¹Department of Chemical and Biochemical Engineering, College of Chemistry and Chemical Engineering, Xiamen University, Xiamen 361005, China

²Engineering Research Center of Marine Biological Resource Comprehensive Utilization, The Third Institute of Oceanography of the State Oceanic Administration, SOA, Xiamen 361005, China

³Department of Chemistry and the MOE Key Laboratory of Spectrochemical Analysis & Instrumentation, College of Chemistry and Chemical Engineering, Xiamen University, Xiamen 361005, China

⁴School of Environment and Energy, Shenzhen Graduate School, Peking University, Shenzhen 518055, China

Correspondence to: Q. Xie (E-mail: qlxie@tio.org.cn) and Z. Xiao (E-mail: xiaozy@xmu.edu.cn)

ABSTRACT: In this study, asymmetric flat-sheet polyethersulfone (PES) nanofiltration (NF) membranes were prepared via immersion precipitation phase inversion with the addition of polyvinylpyrrolidone (PVP). The effects of PVP with the molecular weights (MW) from 17 to 1400 kDa and the concentration from 0 to 3.0 wt % on the morphologies and performances of PES membranes were systematically studied. The prepared membranes were characterized by SEM, AFM, ATR-FTIR, contact angle, membrane porosity, the water flux, and the rejection measurement. The results indicated that the porosity and the hydrophilicity of PES NF membrane increased with increasing PVP concentration, and the hydrophilicity of PES NF membrane also improved with increasing PVP MW. The enhancements of the porosity and hydrophilicity resulted in the higher water flux of PES NF membrane. The rejection of Bordeaux S (MW 604.48 Da) for the prepared PES membrane was increased to above 90% with the low PVP concentration, but it turned to decrease remarkably when the PVP concentration reached to a critical value which related to PVP MW. It was concluded that the addition of a small amount of PVP could significantly increase the permeability of PES NF membrane and maintain its rejection of Bordeaux S above 90%. © 2016 Wiley Periodicals, Inc. *J. Appl. Polym. Sci.* **2016**, *133*, 43769.

KEYWORDS: hydrophilic polymers; membranes; properties and characterization

Received 29 July 2015; accepted 5 April 2016

DOI: 10.1002/app.43769

INTRODUCTION

Nanofiltration (NF) membranes with a weight cut-off (MWCO) of 150 to 1000 Da are widely applied in water and wastewater treatment, pharmaceutical and biotechnology, and food engineering, because of their high flux and good selectivity, relatively low operation pressure and investment.¹ Currently, most commercial NF polymer membranes are thin-film composite membranes prepared via interfacial polymerization. Compared with interfacial polymerization, immersion precipitation phase inversion is a relatively convenient method to prepare asymmetric polymer membranes.

Polyethersulfone (PES) is one of the most popular materials of microfiltration (MF) and ultrafiltration (UF) membranes because of its excellent chemical, thermal, mechanical stability,

and wide pH tolerance. Nevertheless, the hydrophobicity of PES leads to severe membrane fouling in aqueous filtration processes. To improve the hydrophilicity of PES membranes, many modification methods were used which included the use of additives, chemical treatments, grafting, and coating.^{2,3} Among these methods, the addition of hydrophilic polymers, such as polyvinylpyrrolidone (PVP) in the casting solution is the most efficient way. The effects of PVP on the morphologies and performances of PES UF⁴⁻⁹ and PES MF^{10,11} have been extensively investigated. Mohtada and Subir¹² made a brief overview about the effect of PVP on membrane properties, and found inconsistencies in the obtained results. Therefore, it was not straightforward to predict the effect of PVP on the morphology and performance of the prepared membranes based on the previous studies. And the studies of the influence of PVP on the

morphology and performance of PES NF membrane were limited. Boussu¹³ studied the effects of polymer solvents on the permeability and structure of PES NF membrane. The PES NF membrane prepared with *N*-methyl-pyrrolidone (NMP) showed a thinner top skin layer and a higher water flux. Ismail¹⁴ investigated the effect of PVP K30 concentration from 1 to 9 wt % on the morphology and performance of PES NF membrane. The results showed that the water flux linearly increased and the salt rejection linearly decreased with increasing PVP K30 concentration. Zhang¹⁵ also studied the effect of PVP K30 concentration from 3 to 11 wt % on the performance of PES membrane. When the concentration of PVP K30 was 7 wt % the water flux increased to a maximum and then decreased. But the rejection of PEG 1000 decreased with increasing PVP K30 concentration. However, when the PVP K30 concentration changed from 3 to 11 wt %, the obtained PES membranes had MWCO values above 1000 Da and actually belonged to the UF membrane classification.

In the present study, the asymmetric PES NF membranes were prepared with PVP as a hydrophilic additive. The PVP molecular weight (MW) and concentration were able to adjust the thermodynamics and kinetics in the casting solution, which is helpful to control the morphology and performance of PES membrane.¹² To improve the flux and rejection of the PES NF membrane, the effects of the PVP MW from 17 to 1400 kDa and the PVP concentration from 0 to 3.0 wt % on the morphologies and performances of PES membranes were systematically investigated in this study.

EXPERIMENTAL

Materials

PES (Ultrason[®] E6020P, BASF, MW = 51 kDa) was dried at 120 °C for 5 h before using. Three kinds of PVP (PVP K17 with MW = 9 kDa, PVP K30 with MW = 50 kDa, PVP K90 with MW = 1400 kDa) produced by BASF were used as hydrophilic additives. The non-woven fabric support (Polyester, 05TH-100H) was purchased from Shanghai (China) JinChun Company. Analytical grade NMP (XiLong Company, China) was used as the polymer solvent. Pure water from a Millipore system (Millipore, France) was used as the coagulation medium. Analytical grade Bordeaux S (BeiJing J&K[®], China; MW 604.48 Da) was used for the rejection test.

Membrane Preparation

As listed in Table I, PES concentration in the casting solutions was fixed at 27.0 wt % and the PVP concentration was adjusted from 0 to 3.0 wt %. At first, PES and PVP were dissolved into NMP by constant stirring for 12 h. Then, the casting solution was placed in a vacuum oven at 40 °C for 6 h to remove the bubbles completely. The degassed casting solution was cast on a non-woven fabric support with a self-made casting knife. The notch of the knife was 200 μm, and the casting speed was 30 mm·s⁻¹. The nascent membranes were immediately immersed into the coagulation bath (pure water at a temperature of 20 ± 1 °C) without any evaporation. After primary phase separation and membrane formation, the membranes were stored in the fresh pure water bath for 24 h to further remove the residual solvent from the membrane. During the period of membrane

Table I. Compositions of the Casting Solutions

Membrane	PES (g)	PVP K17 (g)	PVP K30 (g)	PVP K90 (g)	NMP (g)
Blank	27	0	0	0	73
K17-1	27	0.3	0	0	72.7
K17-2	27	0.6	0	0	72.4
K17-3	27	0.9	0	0	72.1
K17-4	27	1.5	0	0	71.5
K17-5	27	3.0	0	0	70.0
K30-1	27	0	0.3	0	72.7
K30-2	27	0	0.6	0	72.4
K30-3	27	0	0.9	0	72.1
K30-4	27	0	1.5	0	71.5
K30-5	27	0	3.0	0	70.0
K90-1	27	0	0	0.3	72.7
K90-2	27	0	0	0.6	72.4
K90-3	27	0	0	0.9	72.1
K90-4	27	0	0	1.5	71.5
K90-5	27	0	0	3.0	70.0

preparation, the room temperature was maintained at 20 ± 1 °C and the relative humidity was controlled at 40–60%. The viscosities of the degassed casting solutions were measured using a viscometer (Brookfield DV-2) at 20 ± 1 °C.

Membrane Characterization

SEM. The cross sectional morphologies and the top skin layer thickness of PES membranes were inspected by scanning electron microscope (SEM, ZEISS SIGMA, Germany). The dry membrane samples were frozen in liquid nitrogen and snapped. Then, the samples mounted on the sample stands were sputtered with a thin gold layer and viewed with the electron microscope at 15.0 kV.

AFM. An atomic force microscope (AFM, Agilent MI5500) in tapping mode was employed to analyze the morphology and roughness of the membrane surface. Small squares of the prepared membranes (approximately 1 cm²) were cut and glued onto a glass substrate. The membrane surfaces were imaged at a scan size of 2 μm × 2 μm.

ATR-FTIR. The changes in membrane surface chemistry were elucidated by attenuated total reflection fourier transformed infrared spectroscopy (ATR-FTIR, Bruker VERTXE 70 spectrometer). Sixteen scans were taken at 4 cm⁻¹ resolution between 4000 and 500 cm⁻¹. The OPUS 6.5 was used to record the membrane spectra.

Contact Angle. The hydrophilicities of PES membranes were evaluated using a contact angle goniometer (Beijing HARKE SPCAX3, China). Two microlitres of water droplet from a microsyringe was dropped onto a dry flat membrane surface at room temperature. Five contact angles between water drop and the membrane surface were measured to minimize the experimental error.

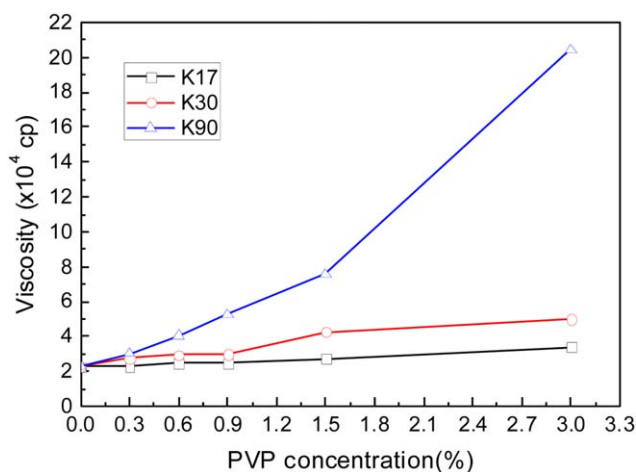


Figure 1. The viscosity of casting solution. [Color figure can be viewed in the online issue, which is available at wileyonlinelibrary.com.]

Membrane Porosity. The membrane porosity ε (%) referred to the ratio between the volume of membrane pores and the total volume of the membrane. It was assumed that all the membrane pores were completely filled with water. Therefore, the membrane porosity could be calculated by the eq. (1)¹⁶:

$$\varepsilon (\%) = \frac{(m_1 - m_2) / \rho_w}{(m_1 - m_2) / \rho_w + m_2 / \rho_p} \quad (1)$$

where m_1 (g) and m_2 (g) were the weights of the wet and dry membranes, respectively, ρ_w was the density of pure water (0.998 g cm^{-3}) and ρ_p was the density of PES (1.37 g cm^{-3}).

Membrane Performances

The water flux and the rejection of Bordeaux S were measured by a stirred dead-end membrane cell (Millipore XFUF07601) with

the effective membrane area 40 cm^2 . The membranes were pre-pressurized under a pressure of 0.6 MPa for approximately 30 min to minimize the compaction effects. Then, the water fluxes and rejections of prepared membranes were measured at 0.6 MPa and $20 \pm 1^\circ \text{C}$. The water flux was calculated by the eq. (2):

$$J = \frac{V}{A \cdot \Delta t} \quad (2)$$

where J was the water flux ($\text{L m}^{-2} \cdot \text{h}^{-1}$), V was the volume of permeate (L), A was the effective area of membrane (m^2), and Δt was the filtration time (h).

An aqueous solution containing 1 g L^{-1} Bordeaux S was used for the rejection test. The rejection (R) was calculated by the eq. (3):

$$R(\%) = \left(1 - \frac{C_p}{C_f}\right) \times 100\% \quad (3)$$

where C_p and C_f referred to the concentrations of Bordeaux S in the permeate and feed, respectively, and were measured with a UV-VIS spectrophotometer (SHIMADZU® UV-1700, Japan).

RESULTS AND DISCUSSION

Viscosity of the Casting Solution

The casting solution viscosity played an important role in the exchange between solvent and nonsolvent during the phase inversion process, which affected the morphology and performance of the final membrane. As shown in Figure 1, the casting solution viscosity increased with the increasing PVP concentration and MW. Especially, the casting solution with PVP K90 showed a more obviously increasing trend due to the huge MW of PVP K90.

SEM

As presented in Figures 2–4, all membranes showed a typically asymmetric structure consisting of a dense skin layer on top

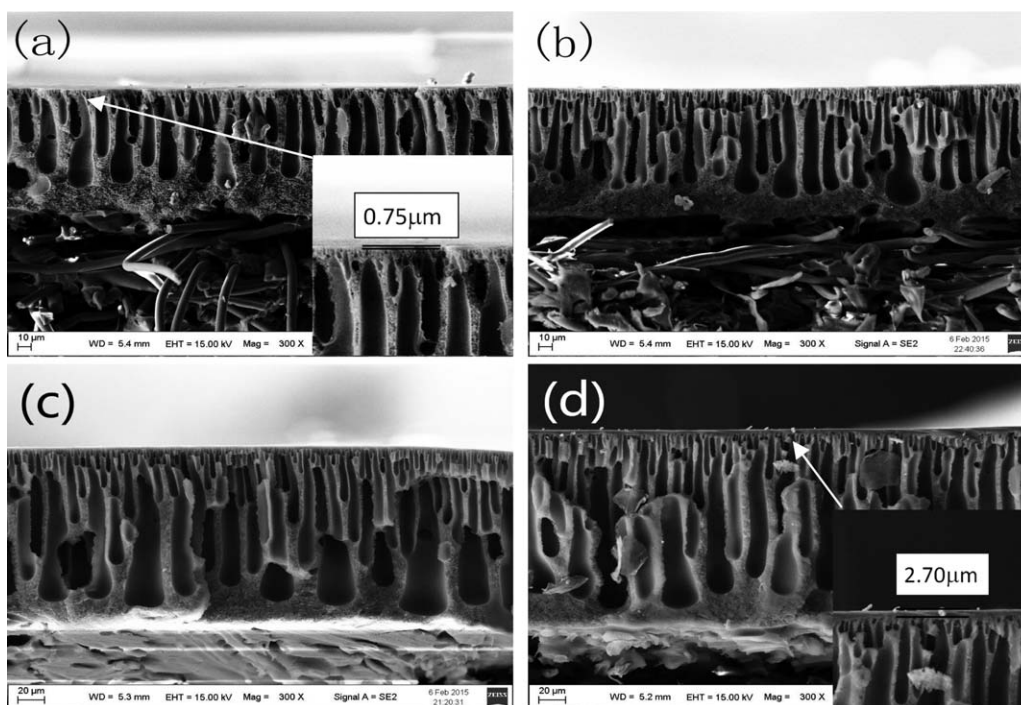


Figure 2. Cross-sectional structures of PES membranes prepared with different PVP K17 concentrations: (a) 0 wt %, (b) 0.3 wt %, (c) 1.5 wt %, (d) 3.0 wt %.

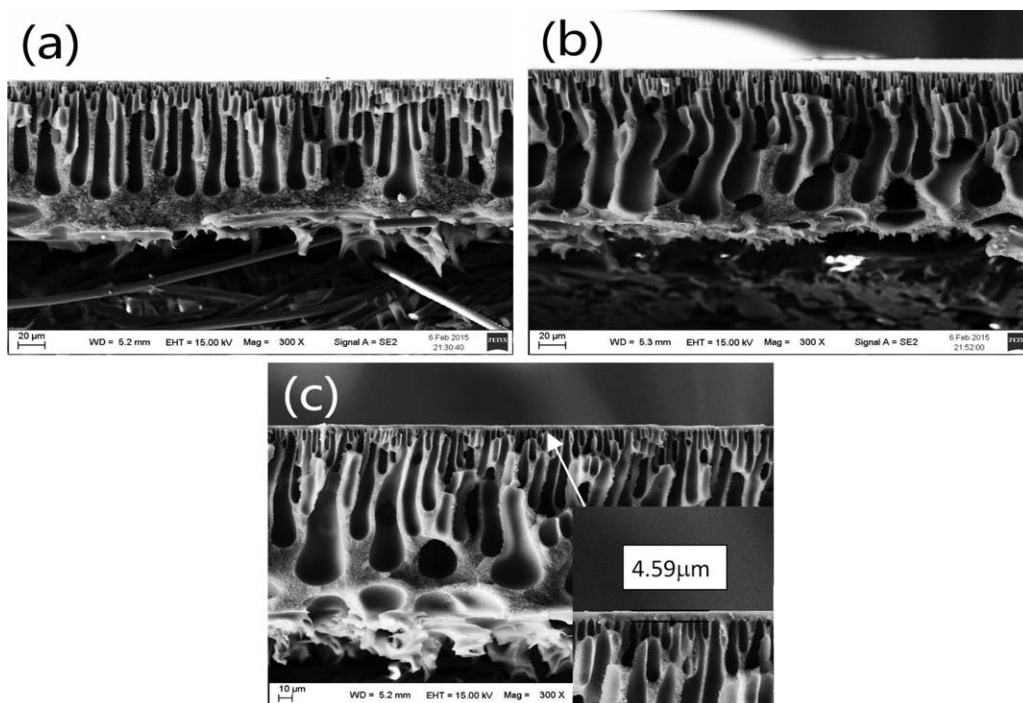


Figure 3. Cross-sectional SEM structures of PES membranes prepared with different PVP K30 concentrations: (a) 0.3 wt %, (b) 1.5 wt %, (c) 3.0 wt %.

and a porous sublayer with finger-like pores. When the PVP concentration increased from 0.3 to 1.5 wt %, the numbers of fine pores beneath the top skin layer and the finger-like pores increased significantly compared with the pure PES membrane. PVP was helpful to form the finger-like pores, performed as excellent pore-forming additives. However, when the PVP concentration increased to 3.0 wt % the top skin layers of three

kinds of PES-PVP membranes became thick. The thickness order of the top skin layers was PVP K90 > PVP K30 > PVP K17, which was consistent with the order of PVP MWs. The casting solution with the higher PVP concentration and MW had the higher viscosity, which led to the delayed demixing in the coagulation bath and the favored formation of a porous substructure with a relatively thick skin layer.¹⁷

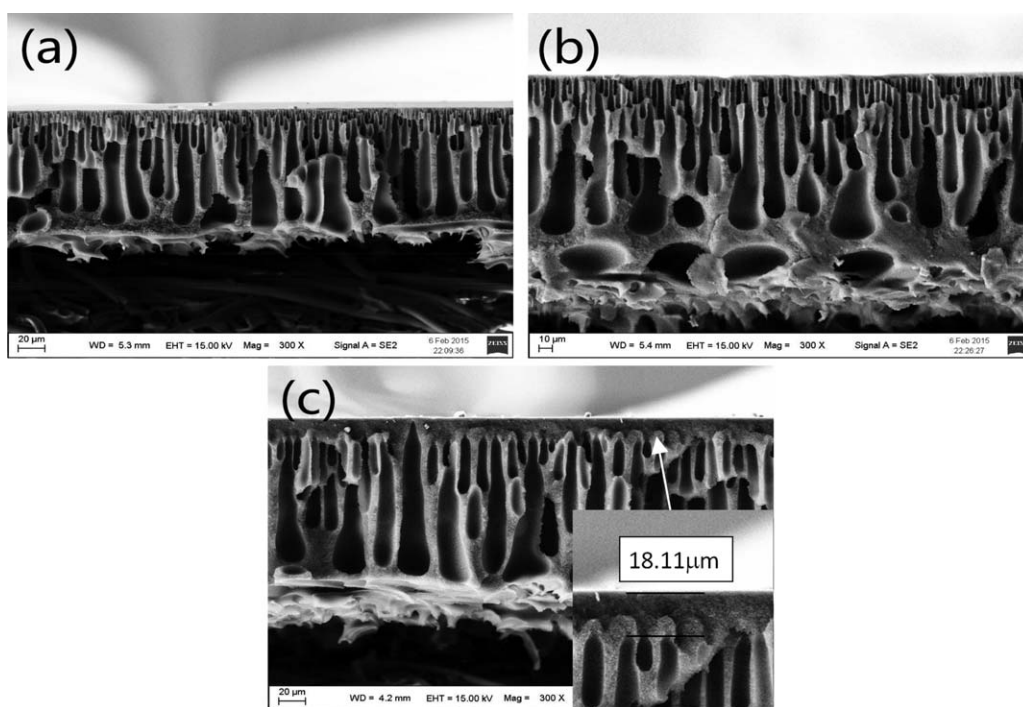


Figure 4. Cross-sectional structures of PES membranes prepared with different PVP K90 concentrations: (a) 0.3 wt %, (b) 1.5 wt %, (c) 3.0 wt %.

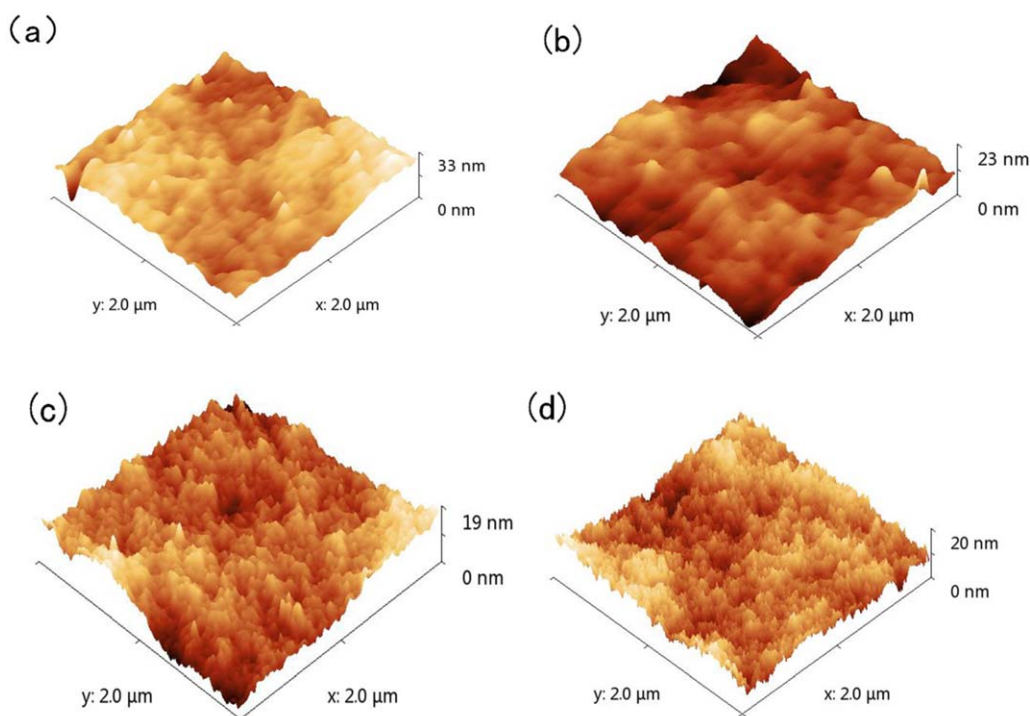


Figure 5. Surface AFM images of PES membranes prepared: (a) without PVP, (b) with 0.6 wt % PVP K17, (c) with 0.6 wt % PVP K30, (d) with 0.6 wt % PVP K90. [Color figure can be viewed in the online issue, which is available at wileyonlinelibrary.com.]

AFM

Figure 5 presented the surface AFM images of PES membranes over a scan area of $2\ \mu\text{m} \times 2\ \mu\text{m}$. The brightest areas indicated the highest points of the membrane surfaces and the dark regions indicated valleys or pores. The roughness parameters of the membrane surfaces can be expressed in terms of the mean roughness (R_a), the root mean square of Z data (R_q), and the mean difference between the five highest peaks and five lowest valleys (R_z).¹⁸

The roughness data and the contact angles were listed in Table II. In contrast to the pure PES membrane, both the roughnesses and contact angles of PES-PVP membranes decreased, which probably resulted from the hydrophilicity of PVP. The membrane surface properties, such as high hydrophilicity and low roughness, were the dominant factors to reduce the membrane fouling.¹⁹ Therefore, the results in Table II indicated PES-PVP membranes

Table II. Roughness and Contact Angles of PES Membranes

Membrane	Roughness			Contact angles
	R_a (nm)	R_q (nm)	R_z (nm)	
PES without PVP	2.88	3.69	23.38	68.3°
PES with 0.6 wt % PVP K17	2.03	2.59	16.16	63.2°
PES with 0.6 wt % PVP K30	1.83	2.45	13.60	58.3°
PES with 0.6 wt % PVP K90	2.14	2.70	14.40	51.2°

had the better antifouling property than the pure PES membrane. Furthermore, PES-PVP membranes prepared with PVP K30 demonstrated the smoothest surface, which might relate to the similar MW between the PES and PVP K30.

ATR-FTIR

According to Figure 6, compared with the pure PES membrane, PES-PVP membranes had a new significant peak at $1664\ \text{cm}^{-1}$ assigned to a primary amide stretch of PVP and the new absorption peaks at $1463\ \text{cm}^{-1}$ and $1438\ \text{cm}^{-1}$ assigned to the bending vibrations of methylene of PVP. Because more PVP remained in the final PES membranes while increasing PVP concentration and MW, it was found that the absorption peak at $1664\ \text{cm}^{-1}$ intensified with increasing PVP concentration and MW.

Membrane Hydrophilicity

As shown in Figure 7, the contact angles of PES membranes showed the same decreasing trend with increasing the PVP concentration and MW. Namely, PES membranes became more and more hydrophilic while increasing the PVP concentration and MW. It was also explained that more PVP remains in the final PES membrane while increasing PVP concentration and MW, which led to be more hydrophilic.

Membrane Porosity

As illustrated in Figure 8, the porosities of PES membranes showed an increasing trend with increasing PVP concentration. When the PVP concentration increased from 0 to 3.0 wt %, the porosity of PES membrane increased from 60.7% to about 71%. The porosity of the PES-PVP K90 membrane was lower than the PES-PVP K30 membrane at the same PVP concentration. Because PVP K90 had a higher MW than PVP K30, it more

easily blocked the void interconnection path and remained in the final PES membrane.

Permeation and Rejection Properties

According to Figure 9, the water flux of the PES-PVP K90 membrane linearly increased with the increasing PVP K90 con-

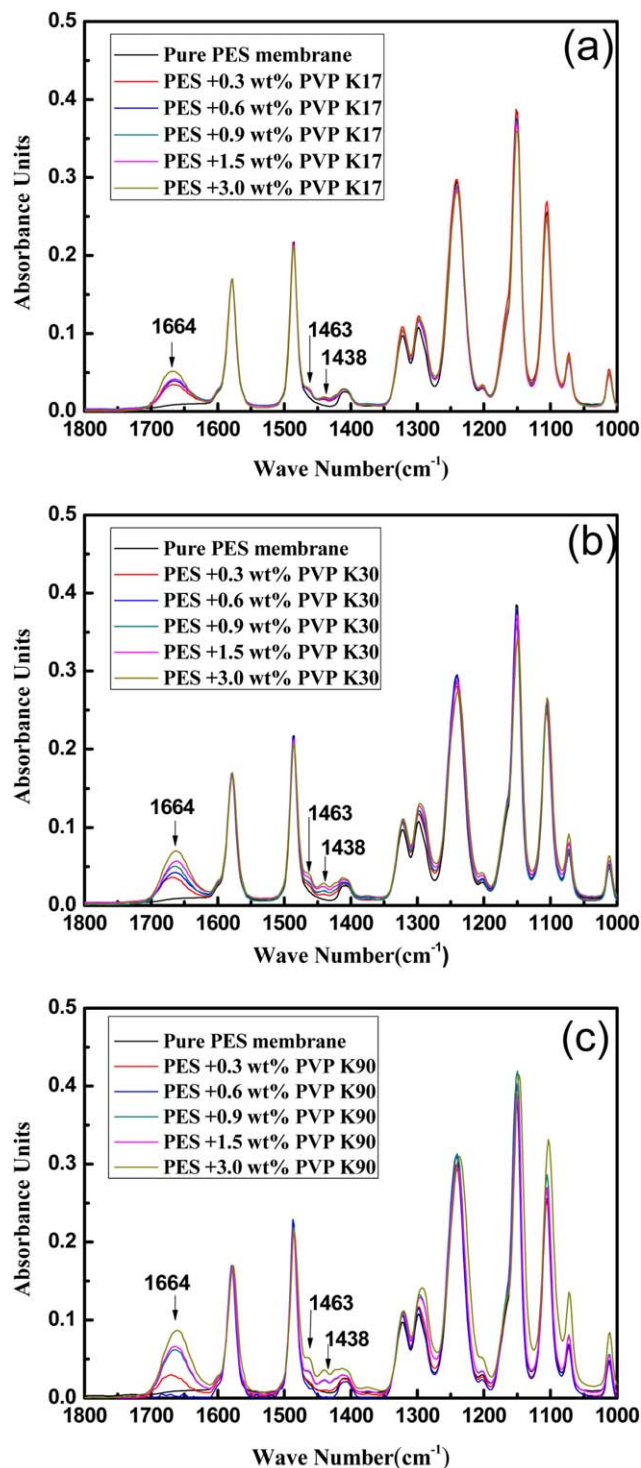


Figure 6. FTIR spectra of PES membranes prepared with: (a) PVP K17, (b) PVP K30, (c) PVP K90. [Color figure can be viewed in the online issue, which is available at wileyonlinelibrary.com.]

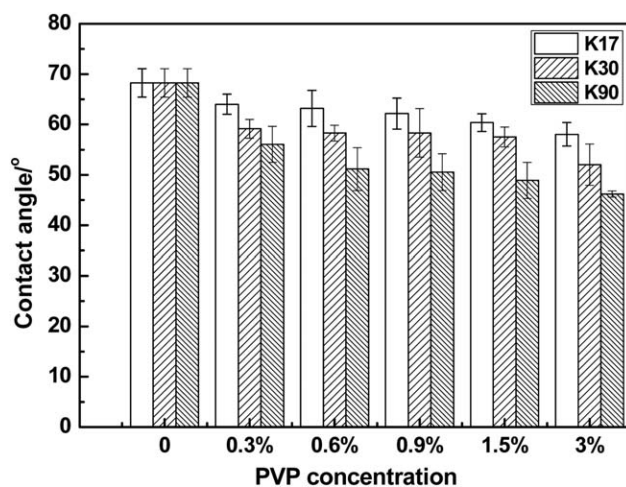


Figure 7. Contact angles of PES membranes prepared with PVP.

centration, but the water flux of the PES-PVP K30 membrane reached a maximum at 0.6 wt % and the water flux of the PES-PVP K17 membrane closed to a maximum at 1.5 wt %. It is well known that the water flux related to the membrane porosity, hydrophilicity and the thickness of top skin layer. In this study, the porosities and hydrophilicities of the PES membranes were enhanced with increasing the PVP concentration, which increased the water flux. But the top skin layer became thicker with the increasing PVP concentration and MW, which decreased the water flux. Although the PES-PVP K30 membrane had the higher porosity and hydrophilicity than the PES-PVP K17 membrane when the PVP concentration reached to 1.5 wt %, the PES-PVP K30 membrane showed the lower water flux due to its thicker top skin layer. In addition, the PES-PVP K90 series membranes showed the lowest water flux among three kinds of PES-PVP membranes, because the PES-PVP K90 membranes had the thickest top skin layer and more PVP K90 remained in the final membrane which blocked the void interconnection path and reduced the pore interconnectivity.^{20,21}

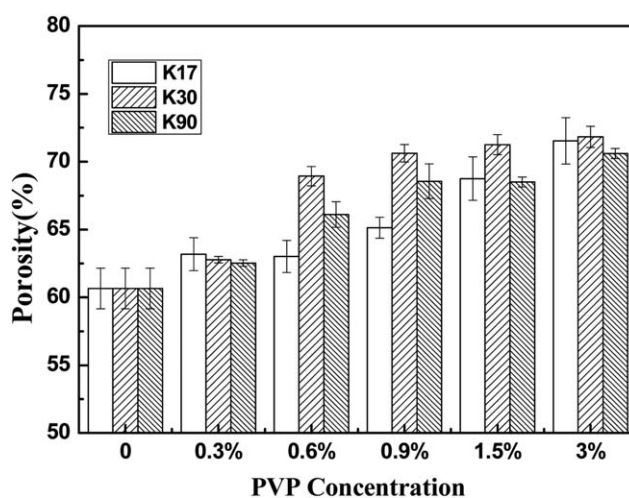


Figure 8. Porosities of PES membranes prepared with PVP.

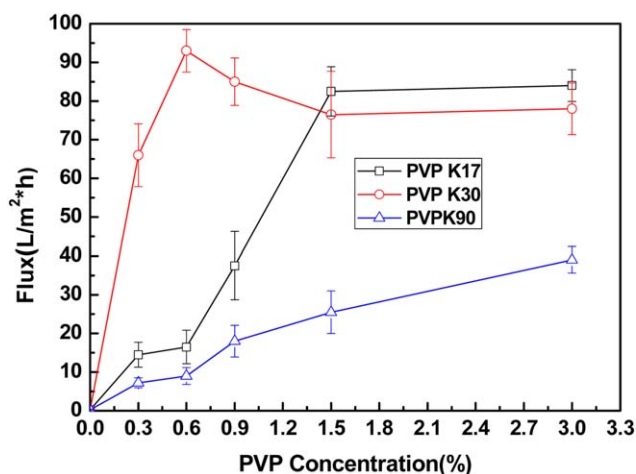


Figure 9. Water fluxes of PES membranes prepared with PVP. [Color figure can be viewed in the online issue, which is available at wileyonlinelibrary.com.]

According to Figure 10, the rejection of Bordeaux S increased greatly from 46% to above 90% when the PVP concentration arose from 0 to 0.3 wt % at a very low content. However, when the PVP K17/PVP K30 concentration increased to 3.0 wt % and the PVP K90 concentration increased to 1.5 wt %, the PES-PVP membranes showed a lower rejection than the pure PES membrane. It was explained that when the PVP concentration was beyond a critical value the PES-PVP membrane tended to form a thicker top skin layer with a more porous structure because of the delayed demixing.

Many studies revealed that PES UF membranes with the higher permeability were expected to have the lower rejection.^{13,22,23} Ismail¹⁴ also reported that PES NF membrane with the higher flux had the lower rejection while increasing the PVP concentration. In this study, it was found that when the PVP K17/PVP K30 concentration increased from 0.3 to 1.5 wt % or the PVP K90 concentration increased from 0.3 to 0.9 wt % the water

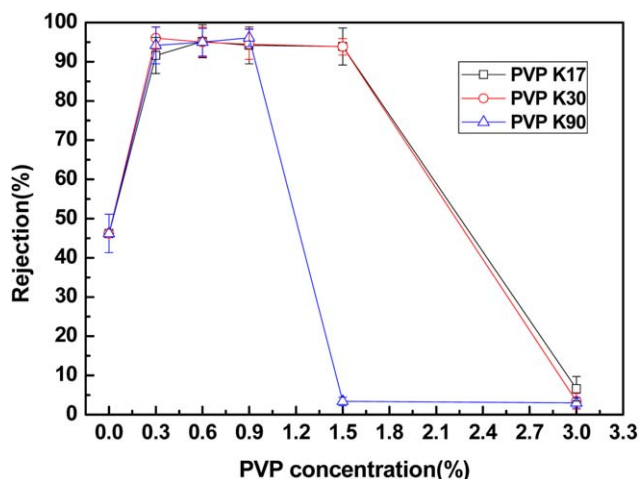


Figure 10. Rejections of PES membranes prepared with PVP. [Color figure can be viewed in the online issue, which is available at wileyonlinelibrary.com.]

flux of the PES-PVP membrane significantly increased without reducing the rejection of Bordeaux S.

CONCLUSIONS

The PVP MW varied from 17 to 1400 kDa and the PVP concentration varied from 0 to 3.0 wt % in the casting solutions exhibited significant effects on the morphologies and performances of PES NF membranes. Both the porosity and the hydrophilicity of PES NF membrane increased with the increasing PVP concentration. The hydrophilicity of PES NF membrane was also enhanced with the higher PVP MW. Both the water flux and the rejection of PES NF membrane were improved with the addition of the low PVP concentration. However, the rejection of PES membrane turned to decrease remarkably when the PVP concentration was beyond a critical concentration which related to PVP MW. It was found that PES NF membranes could be prepared with a small amount of PVP to remarkably increase the permeability without a reduction in selectivity.

ACKNOWLEDGMENTS

The authors gratefully acknowledge for this project sponsored by the Scientific Research Foundation of Third Institute of Oceanography, SOA (No. 2013015), Science & Technology Planning Project of Fujian Province (No. 2014H0027), National Natural Science Foundation Youth Fund of China (No. 21406185), Shenzhen Strategic Emerging Industry Development Funds (JCYJ20140417144423188). The authors are grateful to Prof. James R. Bolton from the Department of Civil and Environmental Engineering at the University of Alberta for his kind assistance with our English writing.

REFERENCES

- Mohammad, A. W.; Teow, Y. H.; Ang, W. L.; Chung, Y. T.; Oatley-Radcliffe, D. L.; Hilal, N. *Desalination* **2015**, *356*, 226.
- Van der Bruggen, B. *J. Appl. Polym. Sci.* **2009**, *114*, 630.
- Ahmad, A. L.; Abdulkarim, A. A.; Ooi, B. S.; Ismail, S. *Chem. Eng. J.* **2013**, *223*, 246.
- Amirilargani, M.; Saljoughi, E.; Mohammadi, T.; Moghbeli, M. R. *Polym. Eng. Sci.* **2010**, *50*, 885.
- Wu, L. S.; Sun, J. F.; He, C. J. *J. Appl. Polym. Sci.* **2010**, *116*, 1566.
- Marchese, J.; Ponce, M.; Ochoa, N. A.; Pradanos, P.; Palacio, L.; Hernandez, A. *J. Membr. Sci.* **2003**, *211*, 1.
- Mosqueda-Jimenez, D. B.; Narbaitz, R. M.; Matsuura, T.; Chowdhury, G.; Pleizier, G.; Santerre, J. P. *J. Membr. Sci.* **2004**, *231*, 209.
- Vatsha, B.; Ngila, J. C.; Moutloali, R. M. *Phys. Chem. Earth* **2014**, *67–69*, 125.
- Al Malek, S. A.; Abu Seman, M. N.; Johnson, D.; Hilal, N. *Desalination* **2012**, *288*, 31.
- Astakhov, E. Y.; Kolganov, I. M.; Klinshpont, E. R.; Tsarin, P. G.; Kalacheva, A. A. *Petrol. Chem.* **2012**, *52*, 557.
- Kim, N.; Kim, C. S.; Lee, Y. T. *Desalination* **2008**, *233*, 218.

12. Sadrzadeh, M.; Bhattacharjee, S. *J. Membr. Sci.* **2013**, *441*, 31.
13. Boussu, K.; Van der Bruggen, B.; Vandecasteele, C. *Desalination* **2006**, *200*, 416.
14. Ismail, A. F.; Hassan, A. R. *Sep. Purif. Technol.* **2007**, *55*, 98.
15. Zhang, Q. R.; Shi, B. L. *Sep. Sci. Technol.* **2009**, *44*, 3876.
16. Dong, C. X.; He, G. H.; Li, H.; Zhao, R.; Han, Y.; Deng, Y. L. *J. Membr. Sci.* **2012**, *387*, 40.
17. Chakrabarty, B.; Ghoshal, A. K.; Purkait, A. K. *J. Membr. Sci.* **2008**, *315*, 36.
18. Singh, S.; Khulbe, K. C.; Matsuura, T.; Ramamurthy, P. *J. Membr. Sci.* **1998**, *142*, 111.
19. Rahimpour, A.; Jahanshahi, M.; Mortazavian, N.; Madaeni, S. S.; Mansourpanah, Y. *Appl. Surf. Sci.* **2010**, *256*, 1657.
20. Wang, D. L.; Li, K.; Teo, W. K. *J. Membr. Sci.* **1995**, *98*, 233.
21. Wang, D. L.; Li, K.; Teo, W. K. *J. Membr. Sci.* **2000**, *178*, 13.
22. Miyano, T.; Matsuura, T.; Sourirajan, S. *Chem. Eng. Commun.* **1993**, *119*, 23.
23. Susanto, H.; Ulbricht, M. *J. Membr. Sci.* **2009**, *327*, 125.

SGML and CITI Use Only
DO NOT PRINT

